XIX IMEKO World Congress
Fundamental and Applied Metrology
September 6–11, 2009, Lisbon, Portugal

ACCURATE PICOSCALE FORCES FOR INSITU CALIBRATION OF AFM

Koo-Hyun Chung, Gordon Shaw, Jon R. Pratt [1]

[1] National Institute of Standards and Technology, Gaithersburg, MD, USA, jon.pratt@nist.gov

Abstract – The force sensitivity of an atomic force microscope is calibrated directly using an in situ realization of primary electrostatic forces ranging from 320 pN to 3.3 nN with accuracy of a few percent. The absolute accuracy of a common atomic force microscope (AFM) force calibration scheme, known as the thermal noise method is evaluated via comparison to the electrostatic calibration. It is demonstrated that the thermal noise method can be applied with great success to yield force measurements with relative standard uncertainties below 5 % after application of a geometric correction factor.

Keywords: Electrostatics, Atomic Force Microscope, Piconewton

1. INTRODUCTION

We report a non-contact calibration procedure using electrostatic forces for determining the force sensitivity of electrically conductive colloidal probes in atomic force microscopes (AFMs). The new method has an advantage over many competing strategies in that it can yield calibration forces that are derived from measurements using units and uncertainties determined by careful application of the definitions and conventions of the Système International d'Unités (SI). Such SI-traceability provides the absolute accuracy necessary for robust, cross-platform accuracy in measurement, and is used here to verify the accuracy and systematic uncertainties associated with a common thermal noise method.

2. METHODS AND PROCEDURES

An electrically conductive colloidal probe was mounted in an AFM equipped with an optical lever and a fixed, micro-electrode as illustrated schematically in Figure 1. The electrostatic force between the colloid sphere and the flat end of the micro-electrode can be expressed as

$$F_e = \frac{1}{2}\frac{dC}{dz_b}\left(U^2\right) \tag{1}$$

where F_e is the electrostatic force acting on the probe, dC/dz_b is the capacitance gradient relative to the motion of the cantilever base, and U is the total electrical potential between the two electrodes. Calculable reference forces can be applied directly to the colloidal probe by applying a voltage to the center conductor of the micro-electrode while the gold coated shield and the colloidal probe are electrically grounded. The change in optical lever voltage ΔV_{OL} for a given change in the applied voltage (electrostatic force) can then be measured, and the optical lever force sensitivity, $OLFS_E$ determined in a straightforward manner.

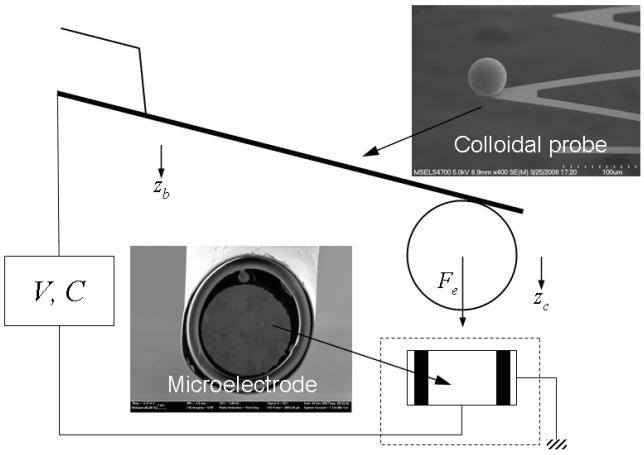

Figure 1. Schematic of experimental setup. Insets show SEM micrographs of devices as constructed.

The general procedure is as follows. First, the capacitance gradient between the colloidal particle and the fixed micro-electrode surface is measured. Second, the combined surface and contact potential that exists between the colloidal particle and micro-electrode is determined. Third, the $OLFS_E$ is computed by applying voltages and recording the changes in optical lever signal, or

$$OLFS_E = \frac{\Delta V_{OL}}{\Delta F_e} \tag{2}$$

where ΔV_{OL} is the change in the a position sensitive photo detector (PSD) signal due to cantilever deflection in V and ΔF_e is the computed change in electrostatic force in N.

The optical lever displacement sensitivity, $OLDS$ can be computed from the $OLFS_E$ using the thermal noise spectrum as proposed by Higgins, et al [1],

$$OLDS = \sqrt{\frac{\pi k f_R P_{dc} Q}{2 k_B T}} \tag{3}$$

where k is the mechanical stiffness of the force sensor, f_R is the resonance frequency, P_{dc} is the direct current (DC) power response of the cantilever, and Q is the quality factor, all of which can be determined from curve fitting of the thermally excited power spectrum of V_{OL}, with k_B being the

Boltzmann constant and T the temperature of the air surrounding the cantilever. We modify Eq. 3 here by noting that the displacement and force sensitivities are related by the stiffness (k=*OLDS/OLFS*), so that

$$OLDS_{ET} = \frac{\pi f_R P_{dc} Q}{2k_B T \cdot OLFS_E} \tag{4}$$

Note that this formulation of the *OLDS* does not contain correction factors to account for the difference between the dynamic mode shape and the static deflection, or for the laser spot diameter and its position along the cantilever [2,3]. These corrections amount to a multiplicative constant within Eq. 4, and can be obtained empirically to improve the absolute accuracy of the *OLDS* as we describe later.

2.1 Micro-electrode. For an ideal sphere-on-flat capacitor geometry, the capacitance gradient and resulting electrostatic force are wholly due to the interaction between the sphere and the flat electrode, so that the force F_e is symmetrically distributed around the sphere and the effective line of action for the force is well approximated by a vector normal to the flat electrode surface and acting through the center of the sphere. For the actual colloidal probe, there is capacitance between the micro-electrode surface and the conductive cantilever to which the colloidal particle is affixed. This background capacitance may cause radial asymmetry in the electrical field between the colloid probe and microelectrode, skewing the force vector. To help avoid this asymmetry, a micro-coaxial electrode was fabricated by encapsulating a gold wire 25 μm in diameter inside a micropipette using epoxy, and then sputter coating the exterior with Cr/Au. The end of the Au coated glass micropipette was cut and polished using Focused Ion Beam milling. As a result, the center gold micro-wire electrode was insulated from the outer conductive Au layer by glass and epoxy. Functionally, the micropipette resembles a rigid coaxial cable with the outer Au layer serving as an electrical shield. Figure 1 shows scanning electron microscope (SEM) micrographs of a representative colloidal probe and microelectrode. Although there is some dimensional asymmetry in the microelectrode, this does not contribute significantly to asymmetry in the electrical field (e.g., the force).

Numerical simulations suggest that this micro-electrode geometry effectively limits the undesirable interaction with the cantilever spring, so that gradients arising perpendicular to z_c are negligible. Attempts to experimentally measure these perpendicular capacitance gradients revealed them to be smaller than could be detected using our equipment.

The capacitance gradient, $dC/dz_b \approx \Delta C/\Delta z_b$, is measured using an accurate capacitance bridge to record the changes in the value of capacitance ΔC while a calibrated displacement sensor records the changes in the displacement at the base of the cantilever, Δz_b, as the probe is moved vertically downward using the AFM's z-axis scan stage. The capacitance is measured at several values of z_b, returning to a home position between each displacement in order to measure and subtract the effects of slow drift in the capacitance, which is small.

2.2 Surface potential determination. After determining the capacitance gradient, the capacitance bridge is replaced with a DC power supply. A constant potential, V_{dc}, is applied while the optical lever voltage is measured. The total potential and the resulting electrostatic force in this case are,

$$F_e = \frac{1}{2}\frac{dC}{dz}\left(V_{dc} + V_s\right)^2 \tag{5}$$

Working from expressions for both the sum and difference of the electrostatic forces resulting from V_{dc} values of constant magnitude but opposite polarities and using Eq. 2 to change from F_e to V_{OL} the following quadratic equation is obtained for the surface potential:

$$V_s = \left|V_{dc}\right| \frac{\left(\sqrt{V_{OL}^+} - \sqrt{V_{OL}^-}\right)^2}{V_{OL}^+ - V_{OL}^-} \tag{6}$$

where, V_{OL}^+ and V_{OL}^- are the PSD voltages that result from the deflection of the cantilever for application of a fixed V_{dc} of alternately positive and negative polarity, respectively. Knowing V_s, the calibration force F_e can be computed using Eq. 5 from the applied V_{dc} values, and the $OLFS_E$ computed using Eq. 2. The $OLDS_{ET}$ can then be computed from the fitted parameters of a thermal noise spectrum, as outlined above.

2.3 Thermal noise method. The thermal noise method uses the equipartition theorem to relate the Brownian motion of a cantilever to its spring constant, k [4], or

$$k_T = \frac{OLDS_C{}^2 2k_B T}{\pi f_R P_{dc} Q} \tag{7}$$

where $OLDS_C$ is the optical lever displacement sensitivity obtained by pressing the colloidal probe against a rigid surface. Once the spring constant is known, the optical lever force sensitivity can be computed using the relationship $OLFS_T = OLDS_C / k_T$.

3. RESULTS

The drift corrected relationship between z_b and capacitance for the colloidal probe is given in Figure 2. No systematic residual due to the linear fit is observed so that the gradient appears constant to within measurement accuracy. The average capacitance gradient from the five different measurements is 0.41 fF/μm ± 0.02 fF/μm where the stated uncertainty is one standard deviation of the mean, and contributions to the uncertainty due to systematic uncertainties in the transfer of the units of length and capacitance were negligible. Throughout the remainder of the paper all uncertainties will be reported in this fashion, unless otherwise noted.

An example plot of the functional relationship between the calculated electrostatic force and the corresponding PSD signal is given in Figure 3. The surface potential, V_s, was determined to be 0.34 V ± 0.03 V. The uncertainty in the measurement of the PSD signal is simply one standard deviation of the mean signal measured for a given force increment. The uncertainty in the applied force is derived by

propagating the measurement uncertainties associated with the capacitance gradient (which is dominant), the applied voltage, and the surface potential through Eq 5. The applied electrostatic forces ranged from 320 pN ± 20 pN to 3.3 nN ± 0.1 nN. The $OLFS_E$ of the colloidal probe was determined to be 300 V/ μN ± 20 V/μN using a linear least squares curve fit to the data of Figure 3, where the estimated uncertainty is again expressed simply as one standard deviation of the mean value of $OLFS_E$ from the five different determinations. From ten thermal noise spectra, the mean value of the $OLDS_{ET}$ was determined to be 7.8 V/μm ± 0.7 V/μm. The spring constant $k_E = OLDS_{ET}/OLFS_E$ was 0.026 ± 0.003.

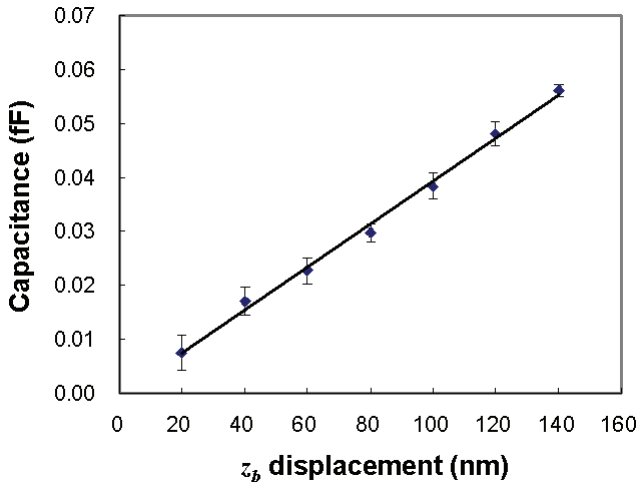

Figure. 2. Capacitance gradient between the spherical electrode at the tip of the colloidal probe and the micro-coaxial cable.

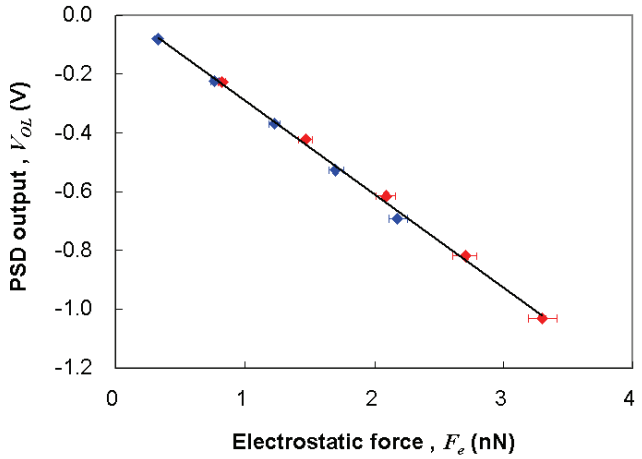

Figure. 3. Sensitivity curve for colloidal probe AFM. Error bars correspond to one standard deviation.

3.1 Empirical corrections for dynamic mode shape and laser spot size. Recall that in determining an expression for $OLFS_T$, correction factors for dynamic mode shape and laser spot size and location along the cantilever portion of the probe were neglected. By combining these corrections together, Eq. 4 can be restated as

$$OLDS_{ET} = \frac{\alpha \pi f_R P_{dc} Q}{2 k_B T \cdot OLFS_E} \tag{8}$$

where α is a multiplicative correction factor that accounts for both the dynamic mode shape and the laser spot size effects. The value of α for the colloidal probe used in the experiments shown in Figures 2 and 3 is 1.05, based on the ratio of the uncorrected $OLDS_{ET}$ to the displacement sensitivity determined by pressing the colloid probe against a rigid surface, $OLDS_c$. This geometric correction factor must also be used in the determination of k_T, or from Eq. 7.

$$k_T = \frac{OLDS_C{}^2 \, 2 k_B T}{\alpha \pi f_R P_{dc} Q} \tag{9}$$

The value of $OLFS_T$ calculated using $OLFS_T = OLDS_C / k_T$, should be corrected upwards by a factor of α. $OLFS_T$ agrees with our estimate of $OLFS_E$ to within measurement uncertainty after this correction is made.

4. CONCLUSIONS

An accurate method of applying picoscale forces directly to the sensing element of atomic force microscopes has been demonstrated. The technique yields traceable primary forces for in situ calibration, avoiding the need for transfer standards or artifacts. Forces ranged from 320 pNs to 3.3 nNs with relative uncertainties of a few percent. The force references were employed to empirically determine correction factors for a convenient and common AFM calibration technique. The correction factors enabled calibration of the AFM via a thermal noise method with relative uncertainty well below the typical 10 % achieved in previous studies [5].

Table. 1 Summary of electrostatic and thermal calibration results

Electrostatic calibration		Thermal calibration	
Capacitance gradient, dC/dz_b (fF/μm)	0.41 ± 0.02	Resonance frequency, f_R (kHz)	2.853 ± 0.001
Magnitude of maximum applied voltage, V_{dc} (V)	3.69	Quality factor, Q	37.4 ± 0.9
Surface potential, V_s (V)	0.34 ± 0.03	DC power response, P_{dc} (V^2/Hz)	5.77×10^{-11} ± 8×10^{-13}
Optical lever force sensitivity, $OLFS_E$ (V/μN)	300 ± 20	Optical lever force sensitivity, $OLFS_T$ (V/μN)	290 ± 10
Optical lever displacement sensitivity, $OLDS_{ET}$ (V/μm)	7.8 ± 0.7	Optical lever displacement sensitivity, $OLDS_C$ (V/μm)	8.2 ± 0.1
Uncorrected stiffness, k_E (N/m)	0.026 ± 0.003	Uncorrected stiffness, k_T (N/m)	0.029 ± 0.001
Corrected stiffness, k_E (N/m)	0.027 ± 0.003	Corrected stiffness, k_T (N/m)	0.027 ± 0.001

ACKNOWLEDGMENTS

The authors would like to thank Dr. Bin Ming and Mr. Richard Kasica from NIST for Focused Ion Beam machining of the micro-electrode. The simulations of micro-electrode performance by Dr. Rae-Duk Lee were also greatly appreciated. We also acknowledge the help of Dr. Chang-Hwa Lee and Dr. Andras Vladar from NIST for SEM images.

REFERENCES

[1] M. J. Higgins, R. Proksch, J. E. Sader, M. Polcik, S. Mc Endoo, J. P. Cleveland, and S. P. Jarvis, "Noninvasive determination of optical lever sensitivity in atomic force microscopy", *Rev. Sci. Instrum.*, vol. 77, no. 1, pp. 013701-1-013701-5, January 2006.

[2] H. J. Butt and M. Jaschke, "Calculation of thermal noise in atomic-force microscopy", *Nanotechnol.*, vol. 6, no. 1, pp. 1-7, January 1995.

[3] R. Proksch, T. E. Schaffer, J. P. Cleveland, R. C. Callahan, and M. B. Viani, "Finite optical spot size and position corrections in thermal spring constant calibration", *Nanotechnol.*, vol. 15, no. 9, pp. 1344-1350, September 1995.

[4] J. L. Hutter and J. Bechhoefer, "Calibration of atomic-force microscope tips", *Rev. Sci. Instrum.*, vol. 64, no. 7, pp. 1868-1873, July 1993.

[5] G. A. Matei, E. J. Thoreson, J. R. Pratt, D. B. Newell, N. A. Burnham, "Precision and accuracy of thermal calibration of atomic force microscopy cantilevers", *Rev. Sci. Instrum.*, vol. 77, no. 8, pp. 083703-1- 083703-6, August 2006.